Pergamon

Int. J. Heat Mass Transfer. Vol. 40, No. 13, pp. 3059–3068, 1997

Printed in Great Britain
0017–9310/97 $17.00 + 0.00

PII: S0017–9310(96)00350–X

Discrete element simulations for granular material flows: effective thermal conductivity and self-diffusivity

M. L. HUNT

Division of Engineering and Applied Science, California Institute of Technology, Pasadena, CA 91125, U.S.A.

(*Received* 5 *February* 1996 *and in final form* 16 *October* 1996)

Abstract—This study uses a two-dimensional discrete-element simulation to determine the effective thermal conductivity and self-diffusivity—quantities that depend on the random motions of particles within a granular material flow. The simulations are performed for solid fractions from 0.015 to 0.68 and for different Biot–Fourier numbers. The assumptions used in the simulations are consistent with dense-gas kinetic theory; hence, the simulation results are shown to compare well with the self-diffusivity based on kinetic theory predictions. For the heat transfer problem, the analysis differs from classic kinetic theory since the particles can exchange heat with the surrounding fluid. For Biot–Fourier numbers much less than 1, the effective conductivity from the simulations coincides with kinetic theory predictions. As the Biot–Fourier number increases above 0.1, the results deviate considerably from the classic analysis, but can be predicted using a modified kinetic theory approach. The simulation is a powerful technique, which can be extended to problems that are not consistent with kinetic theory assumptions. © 1997 Elsevier Science Ltd.

INTRODUCTION

Flows of granular materials describe a class of two-phase flows in which the interstitial fluid plays a negligible role in the mechanics of the flow. Examples include the transport of ore, coal, mineral concentrate, sand, grains, food products, detergents, fertilizers and pharmaceutical tablets. Since viscous drag forces are not important in the flow of the material, much of the recent analytical work has developed from dense-gas kinetic theory [1–3]. In addition, discrete-element simulations, which are similar to molecular dynamics simulations, have been used to study the rheological properties of granular flows [4–7].

Often flows of granular materials are accompanied by associated heat and mass transfer processes such as occurs in the drying, sterilizing, heating or cooling of materials like alfalfa meal, calcium carbonate, coal fines, sewage sludge, lime, soda ash and gypsum [8–12]. Granular flows with heat transfer also occur in rotary kilns [13, 14], which are used for calcination, pyrolysis and sintering of a variety of particulate materials. This current work examines heat transfer processes associated with granular material flows by using both dense-gas kinetic theory and discrete element simulations.

Following the analogy between granular flows and molecular motions, the term *granular temperature* has been used throughout the literature as a measure of the specific kinetic energy of the random motions of the particles [1–3, 15]. Consider for example, the flow of material down an inclined chute. The overall flow rate of the material is associated with the average speeds of all of the particles. However, because the particles collide with other particles and because of local regions of variable particle concentration, the individual particles follow a tortuous path in descending the chute. The granular temperature of this flow would be determined by averaging the squares of the velocity fluctuations in the three directions that the particle can move. An accompanying heat transfer process could be envisioned by considering the chute to be heated to a temperature different than the temperature of the particles that were entering the chute [11, 12]. Associated with this heat transfer process, one would expect to find an enhancement of the thermal conductivity due to the internal mixing of the particles [16, 17]. The focus of this study is the enhancement of the thermal transport due to the mixing within a granular flow.

Although the discrete element simulations have been used to investigate the dynamics of granular flows, it has not been previously extended to heat transfer problems. One important aspect of the heat-transfer discrete-element method is the inclusion of the interstitial fluid. In determining the dynamics of a flow, the interstitial fluid is neglected—as if the particle were colliding in a vacuum. For the heat-transfer process, however, the fluid phase is critical since the particles exchange heat with the fluid. Since the fluid phase is gaseous, the heat capacity is relatively small compared with that for the solid phase. In addition, unlike fluidized beds or suspensions, the motion of the fluid phase results solely from the particle motion.

NOMENCLATURE

A	particle surface area per unit length
$BiFo$	Biot–Fourier number, $\lambda/(\sigma\bar{C})$
c	specific heat of particle
C	velocity
$\bar{C}$	average speed
d	particle diameter
D	self-diffusion coefficient
Δe	internal energy relative to surrounding fluid
$f(\mathbf{C})$	Maxwellian velocity distribution function
$g_0(\nu)$	radial distribution function
h	heat transfer coefficient
k_{kt}	effective conductivity from kinetic theory
k_{sim}	effective conductivity from simulation
l	distance particle travels between collisions
L	length of computational domain
m	mass per unit length
n	particle number density (number per unit area)
N	number of particles
q	heat flux
t	time
T	temperature
t_c	collision interval
u	particle velocity
U	non-dimensional velocity, u/u_m
u_m	average particle speed
x, y	Cartesian coordinates
$\Delta x_i, \Delta y_j$	displacement in i or j direction.

Greek symbols

β	thermal parameter, $u_m\sigma/L$
γ	temperature gradient
λ	mean free path
ν	solid fraction
ρ	density of a particle
φ	angular coordinate
σ	thermal time constant, $mc/(hA)$
θ	nondimensional temperature
τ	time between collisions
Ψ	granular temperature.

Subscripts

f	surrounding fluid
i, j	i or j direction
l	location l
0	initial
x, y	x- or y-component.

Hence, the fluid phase velocities are smaller than the velocities of the solid phase. For this work, the advection of the fluid phase is neglected in comparison to that for the solid phase, but the energy exchange between the particle and the fluid is integral to the analysis.

The first problem that has been considered is simple, the particles have random trajectories, but there is no overall motion of the bed. The particles are perfectly elastic and as a result the kinetic energy of the bed is constant. A thermodynamic temperature gradient is imposed across the bed. The situation is not physically possible and is much simpler than the chute flow example, but it allows for the development of the discrete-element approach and it is consistent with the assumptions involved in the kinetic theory analysis. The purpose is to calculate the rate of energy transferred by the motion of the particles for a range of particle number densities and thermophysical properties. The two important nondimensional parameters are the solid fraction and the particle Biot–Fourier number, which represents for a particle the ratio of the time between collisions to the thermal time constant.

The discrete-element simulation uses a hard-particle model so that the collisions are instantaneous and binary. The temperature of the particle is determined from the solution to the unsteady energy equation for a particle at a uniform temperature. The energy flux is determined by summing the energy brought by all the particles across a slice within the flow. In addition, the simulation is also used to predict the self-diffusion coefficient, which is a measure of the internal mixing of a flow [18–22]. The kinetic theory analysis is used to compare with the numerical simulations and to provide analytical representations for the effective thermal conductivity and the diffusion coefficient. The analysis and follows closely from the earlier results by Hsiau and Hunt [21] and Hsiau [23]. However, the present work concerns two-dimensional systems, since the computation time for three-dimension systems is considerably greater.

KINETIC THEORY ANALYSIS

Following the work by Hsiau and Hunt [21], consider a single particle that is traveling through a fluid with an imposed temperature gradient, γ. The particle Biot number is small, so that the energy equation is a balance between the time rate of change of the internal energy of the particle and the heat transfer rate between the particle and the fluid,

$$mc\frac{\mathrm{d}T}{\mathrm{d}t} = hA(T_f - T) \tag{1}$$

where T is the particle temperature and T_f is the temperature of the surrounding fluid. Unlike the Hsiau and Hunt study, this work considers a two-dimensional system so that m is the mass per unit length of the cylindrical rod and A is the surface area per unit length. The two-dimensional particle has an initial temperature equal to that of the surrounding fluid T_{fo}. The particle moves a distance l from its initial position to a new position in which the fluid temperature has a temperature of $T_{fl} = T_{fo} + l_y\gamma$, where l_y is the y component of l, $l_y = l\cos\varphi$ and φ is the angle with the y-axis. Assuming that the particle travels in the y-direction at a constant speed C_y the particle's temperature at the new position is

$$T = T_{fl} - C_y\sigma\gamma\{1 - \exp[-l_y/(\sigma C_y)]\} \tag{2}$$

using σ as the thermal time constant, $\sigma = mc/(hA)$. Hence, as the thermal time constant approaches zero, the particle temperature approaches that of the surrounding fluid. The internal energy of the particle relative to the surrounding fluid at the location l is

$$\Delta e = mc(T - T_{fl}) = -mcC_y\sigma\gamma\{1 - \exp[-l_y/(\sigma C_y)]\}. \tag{3}$$

The heat flux in the y direction is found by integrating the product of C_y and the internal energy of the particles over the entire velocity space [21, 23]:

$$q_y = \int n\Delta e C_y f(\mathbf{C})\,\mathrm{d}\mathbf{C} \tag{4}$$

where n is the particle number density and the velocity distribution function, $f(\mathbf{C})$, is the local Maxwellian velocity distribution function. For two dimensions, the Maxwellian term is $f(\mathbf{C}) = 1/(2\pi\Psi)\exp[-C^2/(2\Psi)]$ in which Ψ is the granular temperature [3],

$$\Psi = \frac{1}{2}\int C^2(\mathbf{C})\,\mathrm{d}\mathbf{C}. \tag{5}$$

The velocity space is $\mathrm{d}\mathbf{C} = C\mathrm{d}C\mathrm{d}\varphi$ and $C_y = C\cos\varphi$. After substituting in the expression for Δe, C_y, $f(\mathbf{C})$ and $\mathrm{d}\mathbf{C}$ and integrating over φ from 0 to 2π, the equation becomes

$$q_y = -\frac{nmc\sigma\gamma}{2\Psi}\int_0^\infty C^3\left[1 - \exp\left(-\frac{l_y}{\sigma C B_y}\right)\right] \times \exp\left(-\frac{C^2}{2\Psi}\right)\mathrm{d}C. \tag{6}$$

The non-dimensional parameter $l_y/(\sigma C_y)$ can be simplified to $l/(\sigma C)$. This parameter, $l/\sigma C$, is a ratio of the time between collisions to the thermal time constant of the particles. Since a particle changes velocity when it collides with another particle, Hsiau and Hunt used the characteristic length, l, as the mean free path, λ. In that work, the authors assumed that $\lambda/(\sigma C)$ was small for all particle speeds; hence, for these conditions, the exponential in equation (3) can be expanded for small values of the argument, which results in $\Delta e = -mc\lambda\gamma\cos\varphi$. Using this expression, the equation above can be integrated to find

$$q_y = -\left(\frac{\pi}{8}\right)^{1/2} mnc\lambda\Psi^{1/2}\frac{\mathrm{d}T}{\mathrm{d}y}. \tag{7}$$

The constant $(\pi/8)^{1/2}$ differs from the constant found in Hsiau and Hunt [21], $2\sqrt{2}/(3\sqrt{\pi})$, because the present analysis is for two rather than for three dimensions. Following the Hsiau and Hunt analysis, the mean free path is defined from the product of the mean speed, $\bar{C}$ and the collision interval, t_c. For two dimensions, the mean speed is

$$\bar{C} = (\pi\Psi/2)^{1/2} \tag{8}$$

and the collision interval is

$$t_c = 1/[2\sqrt{\pi}nd g_0(\nu)\Psi^{1/2}] \tag{9}$$

hence, the mean free path is

$$\lambda = \bar{C}t_c = 1/[2\sqrt{2}dng_0(\nu)]. \tag{10}$$

In the above expressions, d is the particle diameter, ν is the solid fraction and $g_0(\nu)$ is the two-dimensional radial distribution function evaluated when the particles are in contact. The work by Jenkins and Richman [3] suggests the use of the following equation:

$$g_0(\nu) = (16 - 7\nu)/[16(1-\nu)^2]. \tag{11}$$

This representation follows from the analysis by Henderson [24], which considered the equation of state for a hard two-dimensional fluid. The Henderson study indicates that the equation of state that corresponds with equation (11) is in good agreement with the equation of state found in two-dimensional Monte Carlo simulations.

Noting that the solid fraction can be determined as follows, $\nu = n\pi d^2/4$ and that $nm = \rho\nu$ where ρ is the density of the solid particles, the two-dimensional effective conductivity from kinetic theory analysis, k_{kt}, non-dimensionalized by $\rho c d\,\Psi^{1/2}$, is as follows:

$$\frac{k_{kt}}{\rho c d\Psi^{1/2}} = -\frac{q_y}{\gamma\rho c d\Psi^{1/2}} = \frac{\pi^{3/2}}{32 g_0(\nu)}. \tag{12}$$

Hence, the non-dimensional conductivity decreases with solid fraction. Using the above definition for solid fraction, the mean free path found in equation (10) can be rewritten as

$$\frac{\lambda}{d} = \frac{\sqrt{2}\pi}{16\nu g_0(\nu)}. \tag{13}$$

If $l/(\sigma C)$ is not assumed to be small, the exponential term in the evaluation of Δe in equation (3) cannot be expanded. However, the integral in equation (6) can be evaluated approximately if certain assumptions are made about the ratio of the characteristic length to the particle speed, l/C. In gas kinetic theory, the mean

free path varies with speed of the molecules, $\lambda(C)$ [25]; however, the ratio of the $\lambda(C)/C$ is not a strong function of the molecular speed. Hence, Hsiau [23] assumed that $l/C \approx t_c = \lambda/\bar{C}$ and used this constant to integrate equation (6). For two dimensions, the result is

$$q_v = -nmc\sigma\Psi\gamma\{1-\exp[-\lambda/(\sigma\bar{C})]\} \quad (14)$$

and using the definitions for λ, $\bar{C}$ and v, the expression for the effective conductivity becomes,

$$\frac{k_{kt}}{\rho c d\Psi^{1/2}} = -\frac{q_v}{\gamma\rho c d\Psi^{1/2}}$$

$$= \frac{v\sigma\Psi^{1/2}}{d}\{1-\exp[-\lambda/(\sigma\bar{C})]\}. \quad (15)$$

Note that the heat transfer coefficient has been assumed to be independent of the speed of the particle. The parameter, $\lambda/(\sigma\bar{C})$, is referred to as the Biot–Fourier number (*BiFo*) in Hsiau and Hunt [21]. In equation (15), if *BiFo* is assumed to be much less than one, the non-dimensional effective conductivity is

$$\frac{k_{kt,BiFo\ll 1}}{\rho c d\Psi^{1/2}} = \frac{\sqrt{\pi}}{[8g_0(v)]} \quad (16)$$

which is greater than the expression found in equation (12) by a factor of $4/\pi = 1.273$.

Besides the effective thermal conductivity resulting from the motions of the particles, it is possible to use kinetic theory to calculate the self-diffusion coefficient. Hsiau and Hunt [21] used a method based on the solution of the Boltzmann equation to derive the self-diffusion for granular flows. The same expression was also derived by Savage and Dai [18] by defining the self-diffusion coefficient in terms of the velocity auto-correlation function. The two-dimensional result is included in the thesis by Dai [26] and the subsequent paper by Oger *et al.* [23] and can be written as follows for perfectly elastic disks:

$$\frac{D}{d\sqrt{\Psi}} = \frac{\sqrt{\pi}}{8vg_0(v)}. \quad (17)$$

DISCRETE ELEMENT SIMULATIONS

The discrete element simulations are performed in two parts. The first part is similar to other hard-particle simulations [4–6] in which the position and velocity of each particle in the simulation is calculated and updated throughout the simulation. In addition, the temperature is also calculated in the present simulation. The second part of the simulation uses the temperatures of the particles to calculate the heat flux across the flow due to the random motion of the particles.

In hard-particle simulations, the particle collisions are modeled as binary, instantaneous collisions. Between collisions, particles follow trajectories that are determined from the angle at which the particles collide and from their post-collision speeds. There are no imposed external forces acting on the particles. The present work also assumes that there is no energy dissipated in a collision; hence, the equation for the dynamics of an encounter are determined by the conservation of kinetic energy and linear momentum, which are the same relations used in the kinetic theory of gases [25].

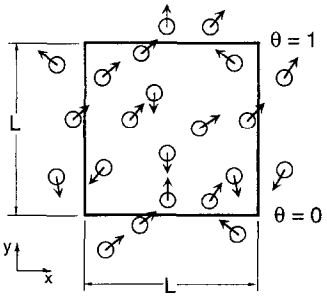

Fig. 1. Computational cell with periodic boundaries (not all of the periodic images are shown).

Figure 1 is a representation of the computational domain containing N particles. The computational domain is square of size L by L and the origin of the x–y coordinate system is placed in the lower left-hand corner. The particles have velocities u_x and u_y. One half of the particles are initially assigned random x and y velocities with values between -0.5 and 0.5. The other half of the particles are given velocities opposite in sign, but equal in magnitude to the first group of the particles. This initial state ensures that their is no net motion of the particles. Hence, the sums Σu_x and Σu_y over all N particles are zero. The velocities u_x and u_y are nondimensionalized using the average speed, u_m, so that $U_i = u_i/u_m$ where u_m is calculated from the average of the square-root of the sum of the velocities squared, $u_m = [\Sigma(u_x^2+u_y^2)^{1/2}]/N$. The initial nondimensional temperatures of the particles, $\theta = [T-T(y=0)]/[T(y=L)-T(y=0)]$, are randomly assigned values between 0 and 1.

As a particle travels, the temperature of the particle can be determined from the solution of the unsteady energy equation as given in equation (1). As in the kinetic theory analysis, a temperature gradient is imposed in the y-direction. If the particle's last y-position and temperature are y_1 and θ_1, the non-dimensional temperature of a particle travelling at a y-velocity u_y after some time τ is as follows:

$$\theta(x,y) = \left(\theta_1 + \frac{u_y\sigma}{L} - \frac{y}{L}\right)\exp\left(-\frac{\tau}{\sigma}\right) + \frac{y_1}{L} + \frac{u_y(\tau-\sigma)}{L}. \quad (18)$$

Furthermore, since the particle travels at a constant velocity between collisions, the time τ, is determined by $\tau = (y-y_1)/u_y$. Introducing the non-dimensional velocity, $U = u/u_m$ and the parameter $\beta = u_m\sigma/L$, the equation above can be rewritten as

$$\theta(x,y) = (\theta_1 + U_y\beta - y/L)\exp[(y_l - y)/(LU_y\beta)] + y/L - U_y\beta. \quad (19)$$

The current program is commenced by specifying the dimensions of the computational cell, the particle diameter, the number of particles within the cell, the thermal parameter β and the total time for the computational run. The program initializes the temperatures and speeds of the particles. Based on the initial velocities and positions of the particles, the program computes the time that each of the N particles collides with another particle. These possible collisions are then ordered into a collision list with the first entry corresponding to the collision that occurs after the shortest period of time. In this manner, the incremental steps are determined by the collision times and are not set as an input parameter to the program. The collision list is then updated and reordered after calculating the next collisions for the two particles that were involved in the initial collision. The program continues by following the collision list and updating and reordering collisions. The program concludes when the total time (the sum of all of the collision times) exceeds the maximum time specified as an input parameter. Similar to other discrete element programs, the computational algorithm can be modified to allow for a variable coefficient of restitution (ratio of rebound speed to impact speed) and a nonzero coefficient of friction [4–6].

Both the x and y boundaries are periodic. Hence, a particle leaving the top ($y = L$) with velocities u_x' and u_y' is reintroduced at the bottom ($y = 0$) with the same x and y velocities, u_x' and u_y'. Similarly, for particles leaving either the bottom, left or right sides of the computational cell. For the temperature field, the periodic conditions are slightly different. If a particle leaves the right or left side, it is reintroduced at the opposite side with the same temperature. However, to impose a temperature gradient in the y-direction, when a particle leaves the top with temperature θ', it is reintroduced at the bottom with a temperature, $\theta' - 1$; if it leaves the bottom at temperature θ'', it is reintroduced at the top with temperature $\theta'' + 1$.

The program proceeds by calculating all collisions that occur over the specified time period. The information that is stored at each collision is the time of the collision, the particles that are involved in the collision, the particles' x and y locations, velocities and the particles' temperatures. This information is then used as input to the second program, which calculates the effective thermal conductivity of the flow. The computational cell is divided into several horizontal slices. The heat transferred across the slice is used to determine the effective thermal conductivity based on results from the discrete element simulation. The heat transferred across a slice is as follows:

$$-k_{\text{sim}} L\gamma\Delta t = \sum_{\text{below}} (\Delta e) - \sum_{\text{above}} (\Delta e) \quad (20)$$

where Δt is the time period over which the sum is calculated. The first sum is done for particles that cross the horizontal slice from below and the second is for particles that cross the slice from above. As in equation (3), Δe is the energy per particle, which is evaluated relative to the temperature at the y-location of the horizontal slice.

The diffusion coefficient can also be evaluated from the simulation. Savage and Dai [18] and Campbell [19] both studied diffusion for a three-dimensional system with an overall shear. Campbell used two methods: a particle tracking technique and a method based on the velocity correlation and found that the two techniques gave very similar results for solid fraction up to 0.5. Savage and Dai also used the velocity correlation method. In the present work, the particle tracking method is used because the method does not require any additional calculations. The diffusion coefficient tensor D_{ij} is defined from the following equality for long times,

$$D_{ij} = \lim_{t\to\infty} \langle \Delta x_i \Delta x_j \rangle / (2t). \quad (21)$$

Hence, D_{xx}, D_{yy} and D_{xy} can be calculated by tracking the x and y displacement over an appropriate time period. Since there is no difference between the x- and y-directions, the corresponding diffusion coefficients should be approximately equal. In addition, the D_{xy} coefficient should approach zero for long times.

RESULTS

The discrete element simulations were performed on a square control volume. For the lowest solid fraction ($\nu = 0.015$), the length of the cell was 50 particle diameters and the number of particles was 50; for the highest solid fractions the cell length was reduced to 10 particle diameters with 70 particles for $\nu = 0.55$, 80 particles for $\nu = 0.63$ and 86 particles for $\nu = 0.68$. The total time of the simulation depended on the solid fraction and the mean speed of the particles. The simulation was considered complete when the effective conductivity reached a value that did not vary considerably ($\pm 5\%$) with time. For the lowest solid fraction the total computational time divided by the average time between a collision (or average number of collisions per particle) was approximately 1200. For the highest solid fraction, the ratio of the total time to the time between collisions was increased to approximately 30 000.

Figure 2 shows the results for the variation in the average mean free path divided by a particle diameter from the simulation, and compares with the kinetic theory result given in equation (13). The results from the simulation appear to follow exactly the kinetic theory predictions. The close agreement parallels the results by Henderson [24], which indicates close agreement between the approximate equation of state based on equation (11) and the exact result.

The diffusion coefficients were calculated by using

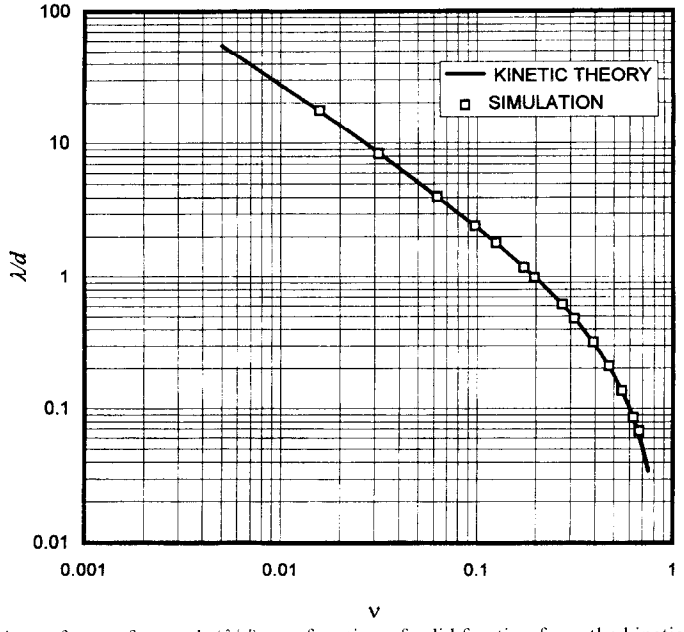

Fig. 2. Comparison of mean free path (λ/d) as a function of solid fraction from the kinetic theory analysis and the discrete element simulations.

the particle tracking method. Figure 3 shows a typical result of the average of the square of the particle displacements from their initial position in both the x and y directions, $\langle(\Delta x)^2\rangle$ and $\langle(\Delta y)^2\rangle$, as functions of time. The solid lines represent a least-squares fit to the data, and the lines are not forced through the origin. The diffusion coefficients, D_{xx} and D_{yy}, are then determined from the slope of the line as given by equation (21). In addition, the value for the coefficient D_{xy} was also calculated. This coefficient was always an order of magnitude smaller than the values for D_{xx} and D_{yy}. The magnitude of the coefficient also appeared to decrease as the computation time increased, which suggests that for a sufficiently long computation, the coefficient should approach zero. The non-dimensional self-diffusion coefficients, $D_{xx}/d\Psi^{1/2}$ and $D_{yy}/d\Psi^{1/2}$, are presented in Fig. 4. Also shown are the results from the kinetic theory, equation (17). Again, the agreement is good between the simulations and the experiments. It is interesting to note that in Savage and Dai [18] the three-dimensional simulation results for the self-diffusion coefficient are compared with the results from the kinetic theory. The comparison shows that the self-diffusion coefficients from the simulations are larger than the kinetic theory predictions and the difference increases with solid fractions. In these simulations, there is an overall motion of the particles because of the imposed shear, the shear flow introduces an anisotropy to the flow and results in preferred collision angles as shown by the simulations of Campbell and Brennen [3]. The result of the shear is to increase the self-diffusion coefficient from an unsheared flow, with the diffusion coefficient in the direction of the imposed flow being the largest. In the kinetic theory analysis, the analysis assumes molecular chaos, which means that random motions of particles are independently distributed. This assumption certainly breaks down for sheared systems in which the collisions are anisotropically distributed [15].

The results for the effective thermal conductivity are presented in Fig. 5. The value for the effective thermal conductivity determined by the discrete element simulations [results from equation (20)] is non-dimensionalized by the value predicted by the kinetic theory result given in equation (16), $k_{\text{sim}}/k_{\text{kt},BiFo\ll 1}$. The ratios of the effective conductivities are presented in terms of solid fraction and Biot–Fourier number. The figure clearly shows that for $BiFo$ greater than 0.1, the effective conductivity begins to decrease significantly from the kinetic theory analysis based on a $BiFo \ll 1$. The simulation also shows that results for the ratios of the effective thermal conductivity does not depend on the solid fraction.

In addition, Fig. 5 also shows the results from the kinetic theory using equation (15) divided by the result in equation (16). The ratio of these two effective conductivities is

$$k_{\text{kt}}/k_{\text{kt},BiFo\ll 1} = [1-\exp(-BiFo)]/BiFo. \quad (22)$$

The results from the simulation appear to be slightly smaller than the result corresponding to equation (22). This difference is probably related to the assumption that the distance a particle travels divided by the speed of the particle, l/C, equals the average collision time defined by $t_c = \lambda/\bar{C}$. Figure 6 presents results from the simulations that indicate the dependence of the time between collisions, l/C, divided by the time between collision for all speeds, $\lambda/\bar{C}$, as a function of the dimensionless particle speeds, $C/\bar{C}$. All of the data

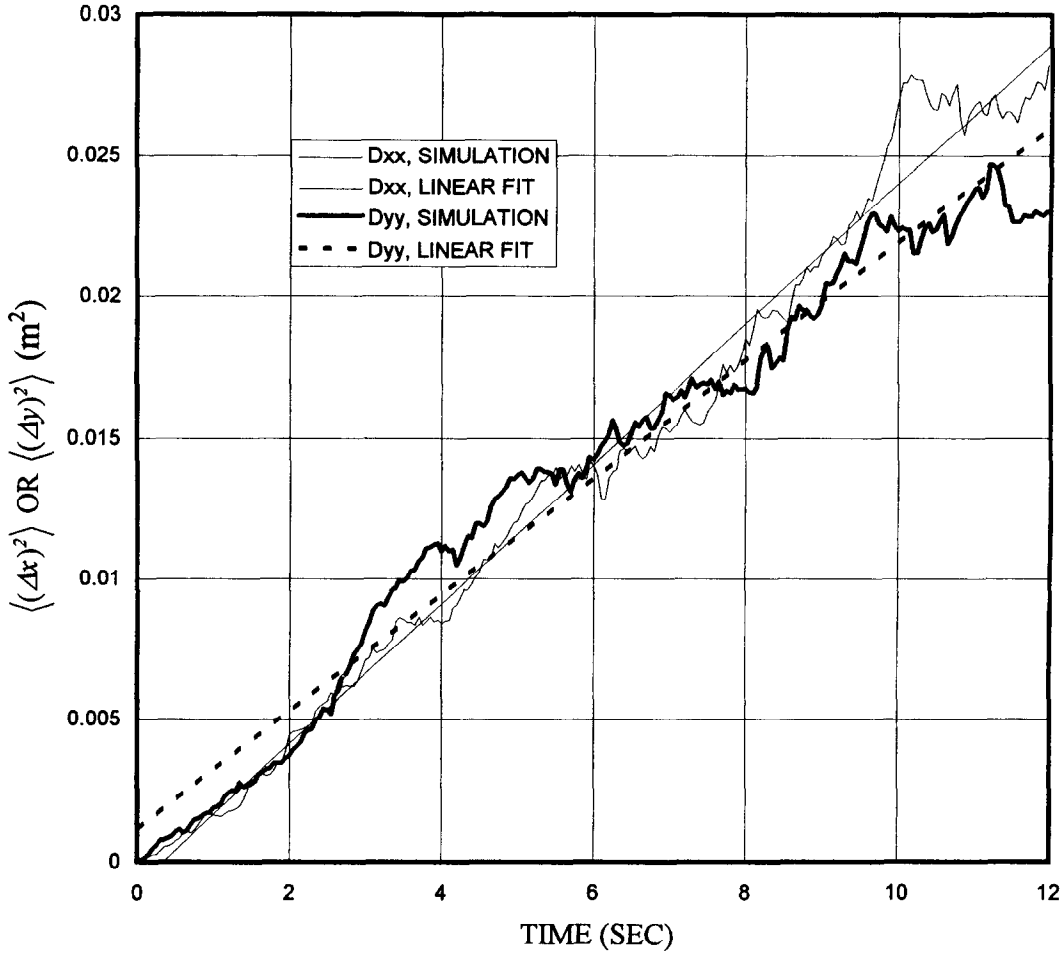

Fig. 3. Mean square deviations in the x- and y-directions over time for a solid fraction of 0.098. The dashed lines are linear fits through the data.

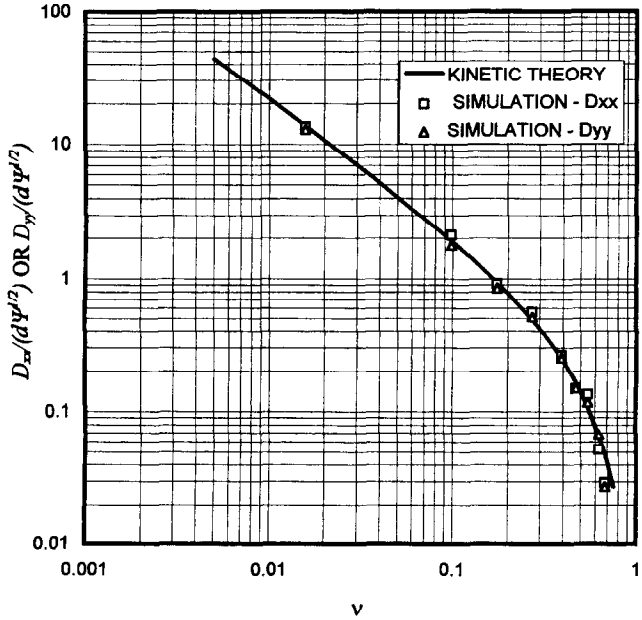

Fig. 4. Comparison of diffusion coefficients in the x- and y- directions ($D_{xx}/(d\Psi^{1/2})$ or $D_{yy}/(d\Psi^{1/2})$) as a function of solid fraction from the kinetic theory analysis and the discrete element simulations.

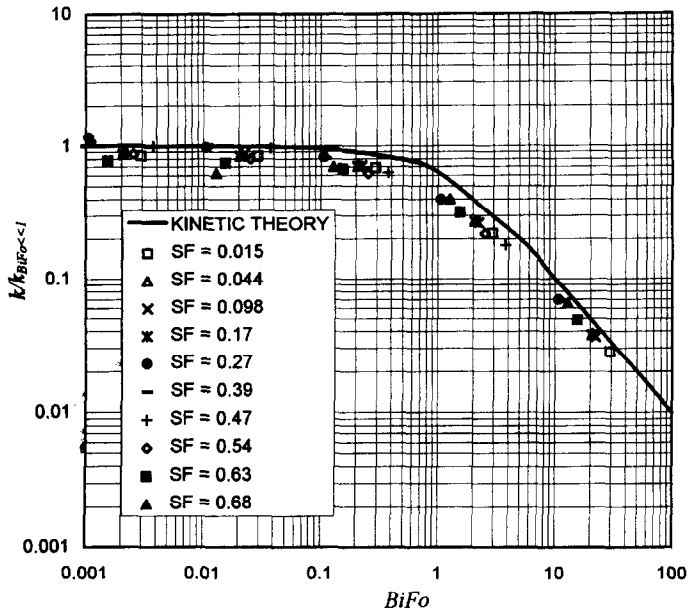

Fig. 5. The effective thermal conductivity as a function of *BiFo* divided by the effective thermal conductivity for $BiFo \ll 1$. The data are also for different values of solid fraction.

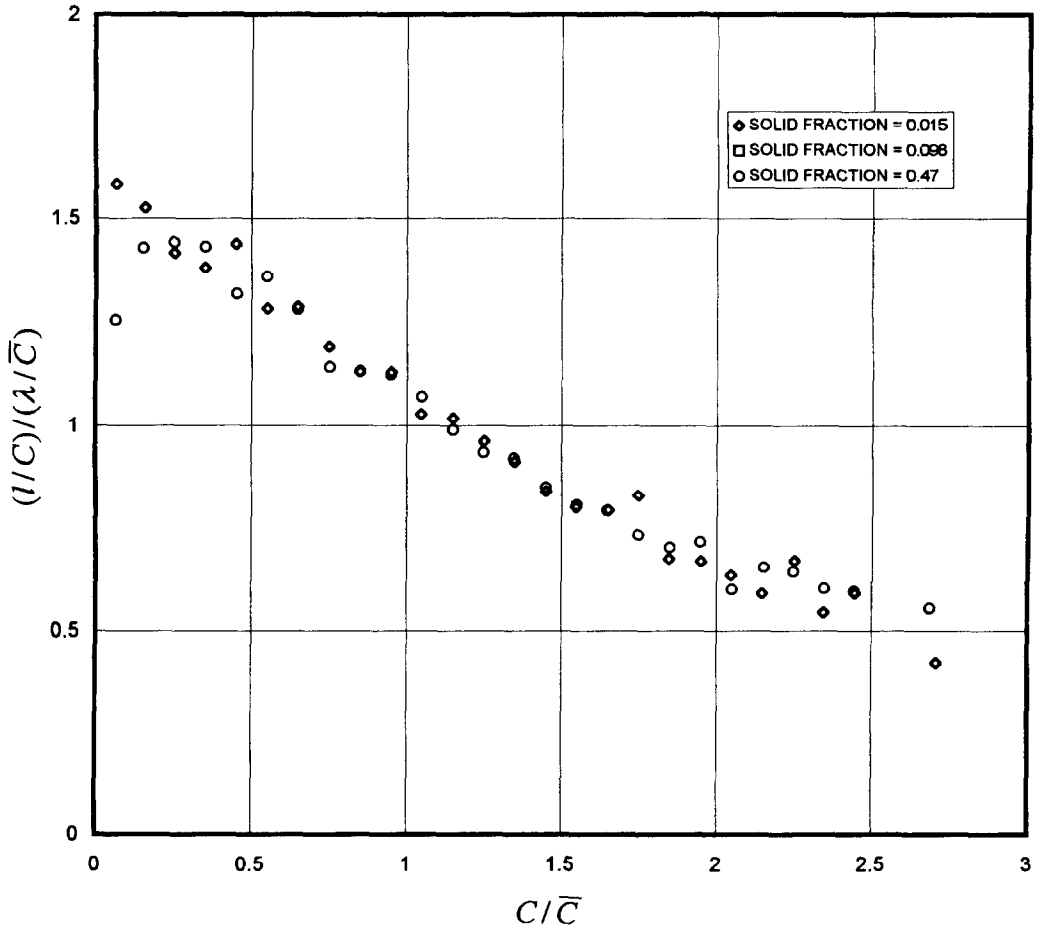

Fig. 6. The time between collisions (l/C) normalized by the mean time between collisions for all particles ($\lambda/\bar{C}$) as a function of particle speed ($C/\bar{C}$).

points represent an average over all particles within a given speed range. In addition, results are presented for three different solid fractions. The results show that the average time between collisions decreases as the speed of the particle increases. Hence, in the integral in equation (6) the term $\{1-\exp[-l/(\sigma C)]\}$ is larger than $\{1-\exp[-\lambda/(\sigma\bar{C})]\}$ for particles with speeds smaller than the average value. The converse is true for particles traveling at speeds larger than the average. However, the integral also contains the term $C^3\exp(-C^2/\Psi)$, which is maximum at $C = 1.22\Psi^{1/2}$. Hence, the value of the integral would be weighted to reflect the faster particles more than the slower particles. As a result, the solution to the integral given by equation (14) would over predict the heat flux and the effective thermal conductivity, which is reflected in the results shown in Fig. 5.

CONCLUSION

This paper presents a method for using a discrete-element model to predict temperatures and effective thermal conductivities for flows of granular materials. The results from the two-dimensional simulation compare well with predictions based on dense gas kinetic theory. The present model makes several assumptions that are consistent with the kinetic theory, but which are not valid for most granular flows. However, many of these assumptions, as mentioned below, could be corrected in future models. In this regard, the present work serves as a benchmark study, which can be used to validate future programs.

In any real flows, there is a driving force to the motion of the particles, such as gravity in flows down inclined chutes or channels, or motion of the bounding surfaces in Couette flows or vibratory flows. The inclusion of an overall flow changes the average motion of the particles and certainly affects the enhanced thermal conductivity. In addition, if there is a driving force, it would also be possible to examine flows with energy dissipation. In state-of-the-art discrete-element simulations, energy dissipation due to inelastic collisions and friction is commonly incorporated into the collision models. However, a new feature would be to include the effect of the energy dissipation in the calculation of the particle temperatures.

In granular flows, the presence of the boundary also critically affects the motion of the particles. Depending on the physical characteristics of the boundary, the particles may roll, slide or bounce off of the bounding surface. Hence, for many granular flows, a slip condition must be used at the boundary. A temperature-slip condition might also be necessary for thermal problems in which the energy is transferred from a bounding surface.

Finally, it might also be possible to consider non-isothermal particles and not rely on the assumption of a small particle Biot number. A simple correction to the model could also account for heat coefficients that vary with particle speed.

REFERENCES

1. Jenkins, J. T. and Savage, S. B., A theory for the rapid flow of identical, smooth, nearly elastic spherical particles. *Journal of Fluid Mechanics*, 1983, **130,** 187–202.
2. Lun, C. K. K., Savage, S. B., Jeffrey, D. J. and Chepurniy, N., Kinetic theories for granular flow: inelastic particles in Couette flow and slightly inelastic particles in a general flowfield. *Journal of Fluid Mechanics*, 1984, **140,** 223–256.
3. Jenkins, J. T. and Richman, M. W., Kinetic theory for plane flows of a dense gas of identical, rough, inelastic circular disks. *Physics of Fluids*, 1985, **28,** 3485–3494.
4. Campbell, C. S. and Brennen, C. E., Computer simulation of granular shear flows. *Journal of Fluid Mechanics*, 1985, **151,** 167–188.
5. Walton, O. R. and Braun, R. L., Viscosity, granular-temperature and stress calculations for shearing assemblies of inelastic, frictionless disks. *Journal of Rheology*, 1986, **30,** 949–980.
6. Campbell, C. S., Computer simulation of powder flows. In *Powder Technology* (ed. K. Iinoya), 1995, Chap. 19.
7. Wassgren, C. R., Brennen, C. E. and Hunt, M. L., A discrete element simulation of a deep bed of granular materials subjected to vertical vibrations. *Physics Review Letters*, 1996 (submitted).
8. Cheremisinoff, P. N., Thermal drying equipment. In: *Handbook of Heat Transfer—Heat Transfer Operations* (ed. N. P. Cheremisinoff), Vol. 1. Gulf Publishing, Houston, 1986, Chapter 37.
9. Malhotra, K. and Majumdar, A. S., Model for contact heat transfer in mechanically stirred granular beds. *International Journal of Heat and Mass Transfer*, 1991, **34,** 415–425.
10. Kunii, D., Chemical reaction engineering and research and development of gas–solid systems. *Chemical Engineering Science*, 1980, **35,** 1887–1911.
11. Spelt, J. K., Brennen, C. E. and Sabersky, R. H., Heat transfer to flowing granular material. *International Journal of Heat and Mass Transfer*, 1982, **25,** 791–796.
12. Patton, J. S., Sabersky,. R. H. and Brennen, C. E., Convective heat transfer to rapidly flowing, granular materials. *International Journal of Heat and Mass Transfer*, 1986, **29,** 1263–1269.
13. Ferron, J. R. and Singh, D. K., Rotary kiln transport processes. *A.I.Ch.E. Journal*, 1991, **37,** 747–758.
14. Cook, C. A. and Cundy, V. A., Heat transfer between a rotating cylinder and a moist granular bed. *International Journal of Heat and Mass Transfer*, 1995, **38,** 419–432.
15. Campbell, C. S., Rapid granular flows. *Annual Review of Fluid Mechanics*, 1990, **22,** 57–92.
16. Wang, D. G. and Campbell, C. S., Reynold's analogy for a shearing granular material. *Journal of Fluid Mechanics*, 1992, **244,** 527–546.
17. Hunt, M. L., Comparison of convective heat transfer in packed beds and granular flows. *Annual Review of Heat Transfer*, 1990, **3,** Chap. 6, 163–193.
18. Savage, S. B. and Dai, R., Studies of granular shear flows—wall slip velocities, layering and self-diffusion. *Mechanics of Materials*, 1993, **16,** 225–238.
19. Campbell, C. S., Self-diffusion in granular shear flows. *Journal of Fluid Mechanics*, 1996 (submitted).
20. Natarajan, V. V. R., Hunt, M. L. and Taylor, E. D., Local measurements of velocity fluctuations and diffusion coefficients for a granular material flows. *Journal of Fluid Mechanics*, 1995, **304,** 1–25.

21. Hsiau, S. S. and Hunt, M. L., Kinetic theory analysis of flow-induced particle diffusion and thermal conduction in granular material flows. *Journal of Heat Transfer*, 1993, **115,** 541–548.
22. Oger, L., Annic, C., Bideau, D., Dai, R. and Savage, S. B., Diffusion of two-dimensional particles on an air table. *Journal of Statistical Physics*, 1996, **82,** 1047–1061.
23. Hsiau, S. S., Kinetic theory analysis of thermal conduction in granular material flows. *Proceedings of the 2nd International Conference on Multiphase Flow '95-Kyoto*, Kyoto, Japan, MOI-7-12, 1995.
24. Henderson, D., A simple equation of state for hard disks. *Molecular Physics*, 1975, **30,** 971–972.
25. Chapman, S. and Cowling, T. G., *The Mathematical Theory of Non-Uniform Gases*, 3rd edn. Cambridge University Press, Cambridge, 1970.
26. Dai, R., Granular flow studies through kinetic theory and numerical simulation approaches. Ph.D. thesis, McGill University, Montreal, Canada, 1993.